Low noise charge injection in the CCD22

David R. Smith[*a], Andrew D. Holland[a], Ian Hutchinson[a], Antony F. Abbey[b],
Peter Pool[c], David Burt[c], David Morris[c]
[a]Brunel University, Uxbridge, Middlesex, UB8 3PH, UK;
[b]Space Research Centre, University of Leicester, Leicester, LE1 7RH, UK;
[c]e2v Technologies, 106 Waterhouse Lane, Chelmsford, Essex, CM1 2QU, UK

ABSTRACT

The inclusion of a charge injection structure on a charge coupled device (CCD) allows for the mitigation of charge transfer losses caused by radiation induced charge trapping defects. Any traps present in the pixels of the CCD are filled by the injected charge as it is swept through the device improving the charge transfer efficiency in the subsequent acquired images. To date, a number of CCD types have been manufactured featuring different methods of charge injection. The e2v Technologies CCD22, used in the EPIC MOS focal plane instruments of XMM-Newton, is one such device and is the subject of this paper. A detailed understanding of charge injection operation and the use of charge injection to mitigate charge transfer losses due to radiation damage in CCDs will benefit a number of planned future space projects, including the ESA GAIA and X-ray Evolving Universe Spectrometry (XEUS) missions.

The charge injection structure and mode of operation in the CCD22 are presented, followed by a detailed analysis of the uniformity and repeatability of the charge injection amplitude across the columns of the device. The effects of proton irradiation on the charge injection characteristics are also presented, in particular the effect of radiation induced bright pixels on the injected charge level.

Keywords: CCD, charge injection, X-ray detector, CTI, proton irradiation

1. INTRODUCTION

The e2v Technologies CCD22 device is a front illuminated three-phase frame transfer device and has been used for X-ray applications in the EPIC MOS focal plane instruments of XMM-Newton[1] and the X-Ray Telescope (XRT) of Swift[2]. The device uses high resistivity silicon and an open-electrode structure to obtain good quantum efficiency between 0.2 keV and 10 keV making it the ideal detector for these instruments. The use of the CCD22 in these space missions means the device has been tested and characterised to a high level and the effects of proton irradiation on the device are well understood[3,4,5]. The device characteristics are summarised in Table 1. A schematic of the CCD22 is shown in Figure 1.

Parameter		*Value*
Active image area		24 × 24 mm
Image section		600 × 600 pixels
Store section		600 × 602 pixels
Pixel size:	Image section	40 × 40 μm
	Store section	39 × 12 μm
Spectral range		0.1 – 15 keV

Table 1. e2v Technologies CCD22 characteristics

[*] David.Smith@brunel.ac.uk; phone +44 (0)189 527 4000; fax +44 (0)189 525 8728; www.brunel.ac.uk

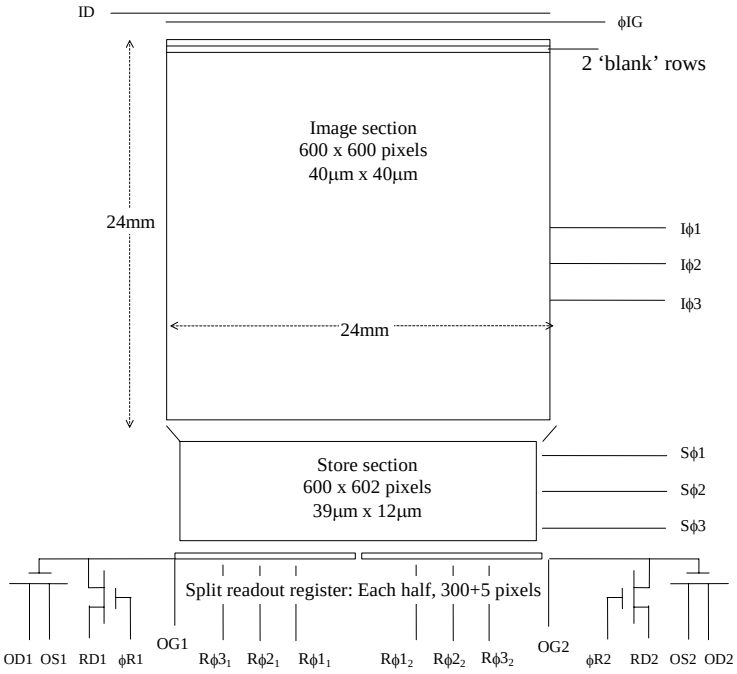

Figure 1. A simplified schematic of the e2v Technologies CCD22

The CCD22 also features charge injection structures to allow the mitigation of radiation induced charge transfer inefficiency (CTI). Charge can be injected into a row at the top of the image section and then swept through the device filling any vacant charge trapping sites and reducing the amount of signal charge lost during readout of the subsequent image. Although the use of charge injection on a CCD22 has been used and observed to significantly reduce CTI in the EPIC MOS cameras of XMM-Newton, there is not much information about the size of the injected charge, the injection uniformity and repeatability and the effects of radiation induced bright pixels on the operation of charge injection. The work presented in this paper describes the preliminary analysis of charge injection operation in a single CCD22 device and characterises these parameters.

1.1. Charge injection

The injection of charge is brought about by pulsing the input gate, ϕIG, while Iϕ1 is also held high. Figure 2 shows a schematic of the charge injection process. Adjustment of the input drain potential, ID, allows fine control of the level of injected charge. The width of the buried channel under the injection gate also controls the level of injected charge.

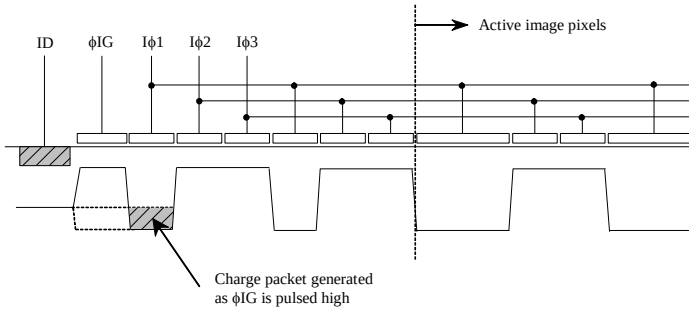

Figure 2. A schematic of the CCD22 charge injection process

2. METHODOLOGY

The CCD22 used for the work presented in this paper was device number B5/21 which had previously been irradiated with protons at Eberhard-Karls-Universität, Tübingen, as part of a radiation damage study to investigate the effect of low energy proton irradiation on the operational characteristics of the device[4]. The device had received ~3.5 × 10^6 protons cm^{-2} to the top half of the image section (1.3 × 10^6 protons cm^{-2} at a mean energy of 170 keV and 2.3 × 10^6 protons cm^{-2} at a mean energy of 330 keV) and ~1.0 × 10^7 protons cm^{-2} (at a mean energy of 70 keV) to the bottom right corner of the image section. The areas irradiated, the proton fluence and the mean energy of the proton beam for each irradiation are shown in Figure 3.

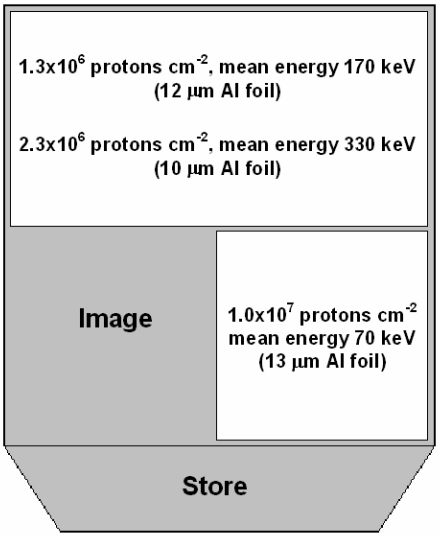

Figure 3. Total fluence and mean proton beam energy for each irradiated section of the CCD

To investigate the charge injection characteristics of the device, the CCD was operated with charge injection occurring continuously, i.e. charge was injected into every row of the CCD on read out. In this way the uniformity of the injection with row number could be investigated along with the uniformity of the charge injection level in each column of the device. The data taken for the analysis presented below were obtained with the device operating at -90 ^oC. The CCD was calibrated using ^{55}Fe X-rays from a Kevex source giving a calibration value of 4.335 eV per channel.

3. ANALYSIS

3.1. Injection uniformity

The CCD image shown in Figure 4 was recorded with ID set to 16.5 volts and ϕIG set to 10.2 volts. The readout node in all the images presented is located at the bottom left corner, i.e. at (0, 0). The background dark current has been subtracted in all the presented plots, unless otherwise stated.

Figure 5 shows the mean charge injection amplitude in each column of the device, panel A, and also the variation in charge injection amplitude along a single column, in this case column 300, in panel B. The standard deviation of the injection level in each column is shown in Figure 6 for all 600 columns of the device. The same data are shown in each panel of the figure, panel B having a smaller vertical scale to emphasise the noticeable dip in standard deviation in the centre of the device. There is also a sharp rise in the standard deviation at the right edge of the CCD indicated in panel A.

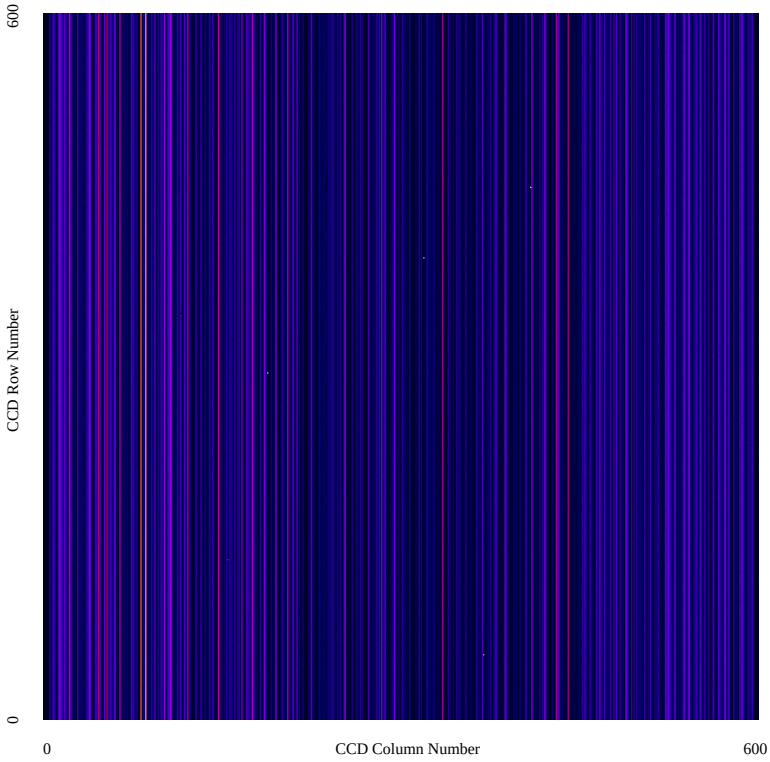

Figure 4. A CCD22 continuous charge injection image taken at -90 ^{o}C

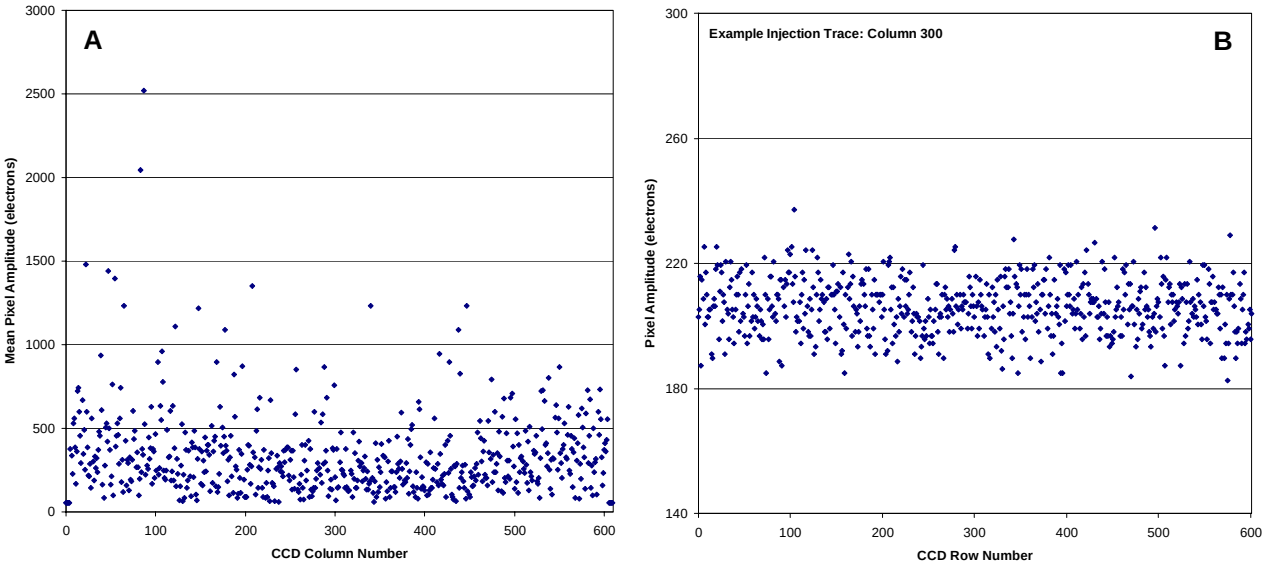

Figure 5. The mean injection amplitude in each column of the device is shown in panel A while panel B shows the variation in charge injection amplitude along a single column

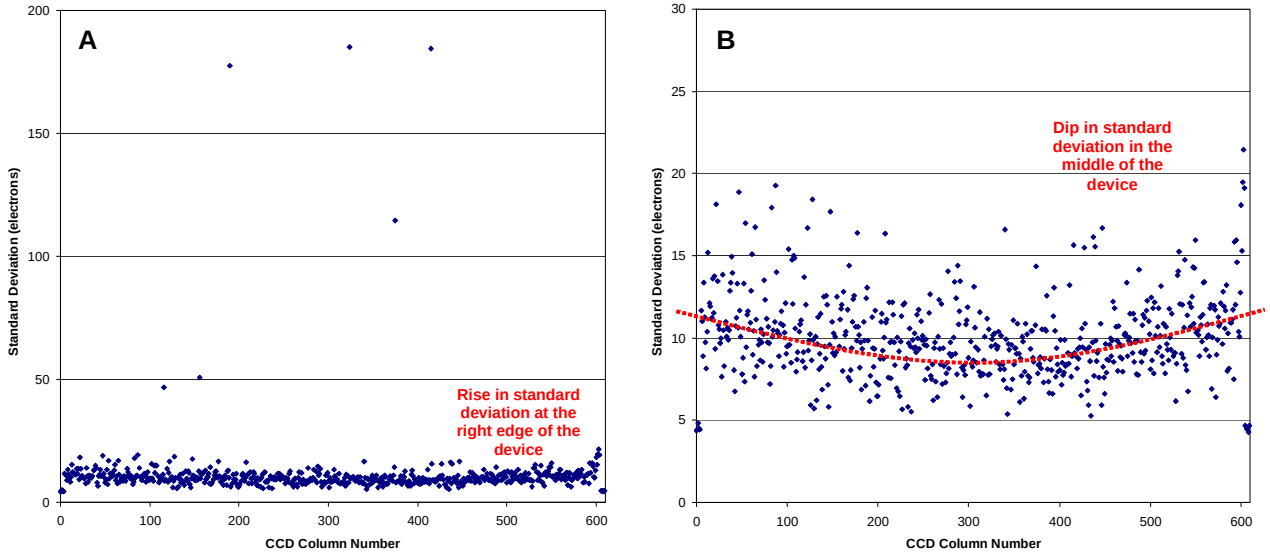

Figure 6. The standard deviation in the charge injection level for each column across the CCD

The standard deviation is plotted against the mean pixel amplitude for each column in the CCD in Figure 7. The square root of an example signal column is shown for comparison. Figure 8 shows a histogram of the measured standard deviations between values of 5 to 15 electrons. This selection was made to remove the <5 electrons standard deviation values, associated with the non-injection columns at each edge of the CCD, and to remove the >15 electrons standard deviation values associated with spurious data points. The data points included in the histogram are indicated in Figure 7. A Gaussian fit to the data points is also shown in Figure 8, with a σ = 1.7 electrons.

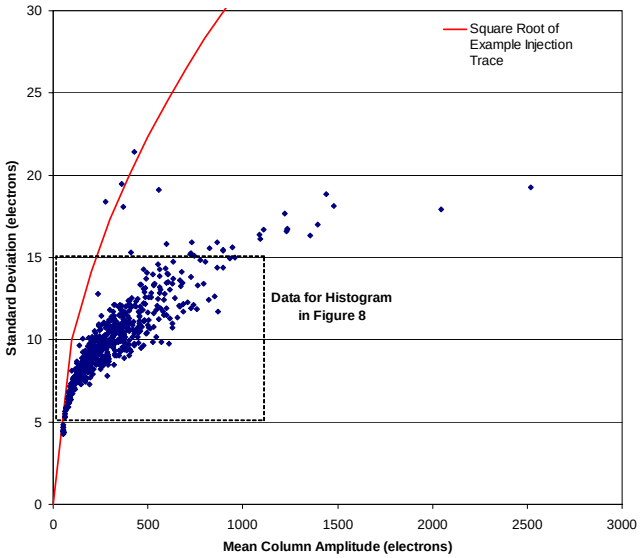

Figure 7. Standard deviation vs. mean column injection amplitude

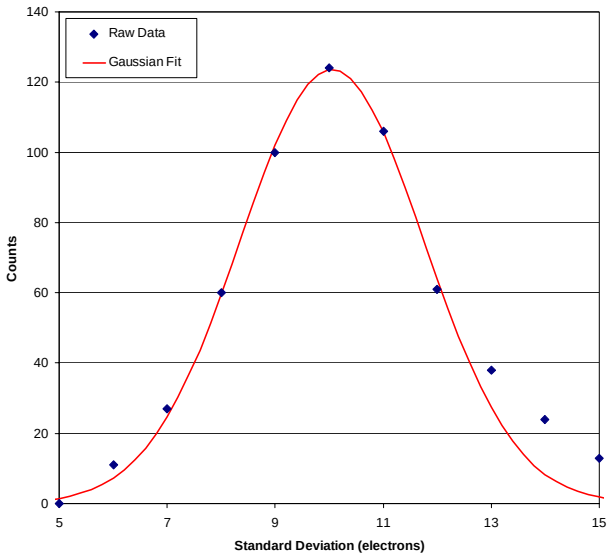

Figure 8. The distribution in the standard deviation of each charge injection column

Figure 9 shows the variation in charge injection amplitude along the length of each of the six columns observed to have a standard deviation >20 electrons. These six columns can clearly be identified in panel A of Figure 6 above. In each of these columns the large standard deviation is the result of a 'spike' in the signal level, after which there is a period of no injection. The length of the column required for the injection level to be regained after the spike varies from no pixels at all, in the case of column 190, to ~150 pixels in the case of column 324. The dark current background level has not been subtracted from the data shown in Figures 9 for better presentation of the 'off' charge level.

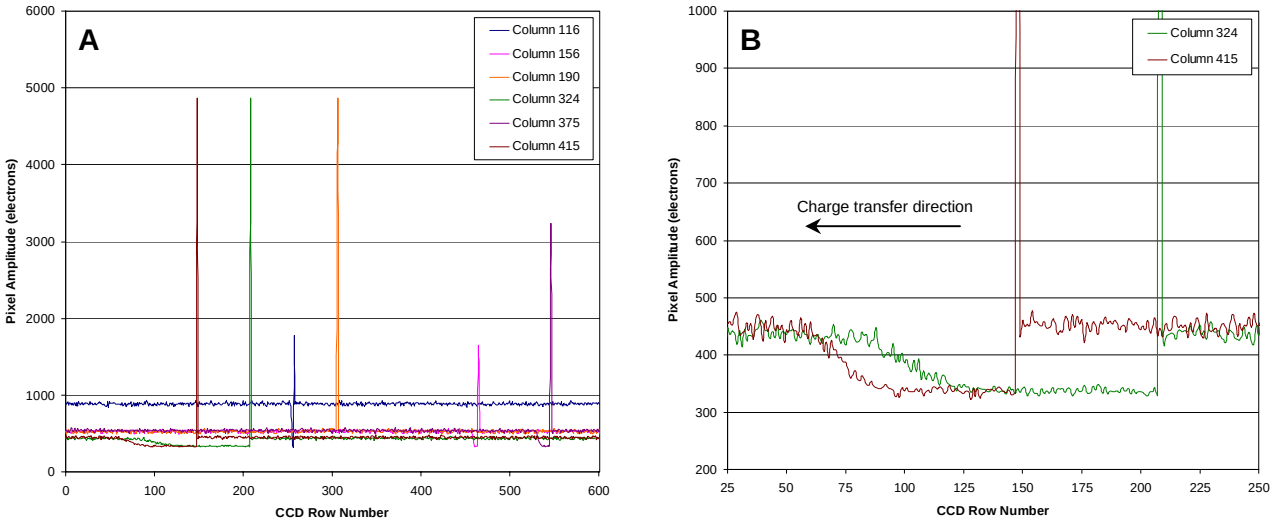

Figure 9. The variation in charge injection level along the length of each of the 6 'spiked' columns

Figure 10 shows the location of the six spikes in the image frame. A non-charge injection frame was examined to see if the six spikes could be linked to bright pixels in the device. Five of the six spikes correlate with radiation induced bright pixels present in the background frame, as shown in panel B of Figure 10. In the sixth case, the spike is most likely linked to a 'Random Telegraph Signal' pixel, the high charge level not being present in the selected background frame[6,7].

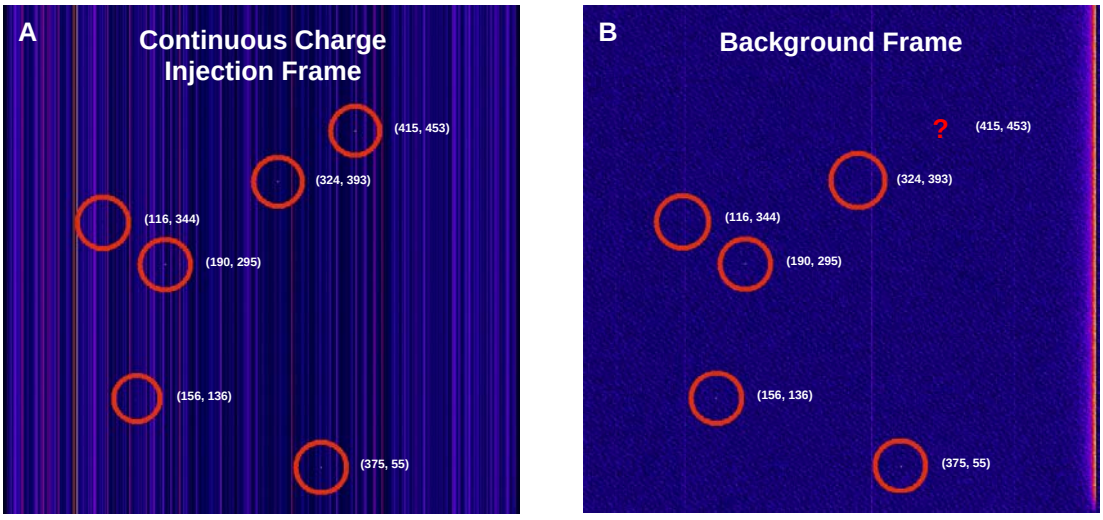

Figure 10. The location of the six injection spikes and their correlation to radiation induced bright pixels

3.2. Injection behaviour with ϕIG

The threshold ϕIG potential for charge injection is approximately ID minus the channel potential and varies slightly for each CCD column. This variation is most likely due to subtle changes in the channel potential at Iϕ1 in each column of the device. Figure 11 shows the how the mean pixel amplitude of 10 CCD columns increases with increasing ϕIG for an ID potential of 16 volts. The distribution of the injection threshold level for the 10 columns shown in the figure is ~0.5 volts. This distribution is representative of all the columns in the device. It can also be seen in the figure that the mean pixel amplitude is a function of the threshold ϕIG potential for a given column, the gain in the mean pixel amplitude being greater for a lower injection threshold.

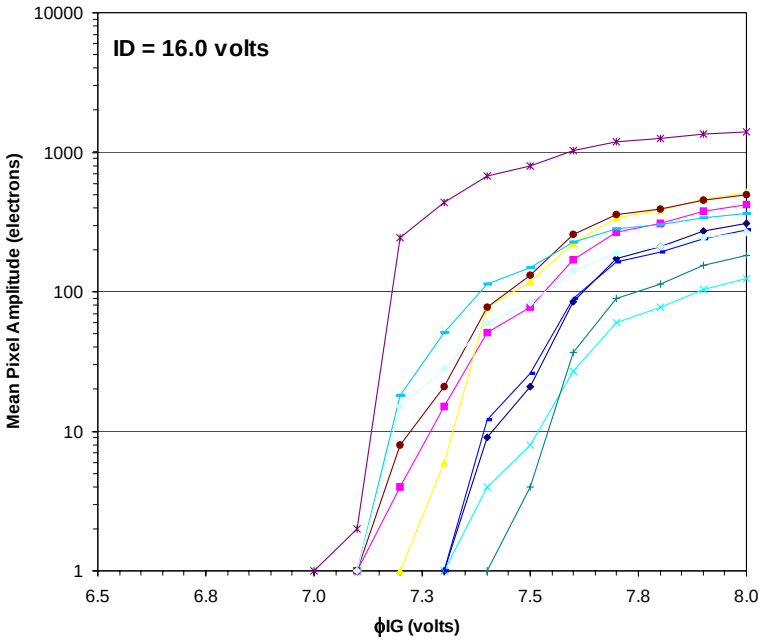

Figure 11. Variation in mean pixel amplitude with ϕIG for 10 CCD columns

4. CONCLUSIONS

This study has shown that for the charge injection mechanism used in the e2v Technologies CCD22 the variation in injection level from column to column is large, ranging from ~330 electrons to ~2500 electrons (i.e. a factor ~7), while the injection level along a given CCD column remains more consistent with a standard deviation in the range of 5 to 20 electrons for a given injection signal. The standard deviation in the injected signal is a lot less than the expected shot noise on the signal, the size of the injected signal being defined by a fixed potential well.

The standard deviation in the injection level along a given CCD column is larger for a higher injection level and increases from the centre of the device to the edges, rising from ~8 electrons to ~12 electrons (i.e. a factor ~1.5). There is also a noticeable rise in the standard deviation in the 6 columns at the right edge of the device. Six columns in the device exhibit a standard deviation >20 electrons, all of which show a pixel amplitude ‘spike’, followed by a period of no injection before the charge injection level returns to the level it was at before the spike. The ‘off’ period varies in length along the column from no pixels at all, column 190, to ~150 pixels in the case of column 324. The presence of a ‘spike’ correlates with the presence of a bright defect within the same pixel in five of the six observed cases. In the sixth case, the spike is most likely linked to a ‘Random Telegraph Signal’ pixel, the high charge level not being present in the selected background frame.

The threshold potential for the onset of charge injection varies across the columns of the devices by ~0.5 volts, the variation most likely being the result of very small changes in the channel potential of each column. After the onset of charge injection, the injection signal level increases with increasing ϕIG, the gain being dependant on the charge injection threshold potential: the lower the injection threshold, the higher the gain.

The presence of radiation induced bright pixels in a device will reduce the effectiveness of charge injection for mitigating CTI as the injected charge may be prevented from reaching the charge trapping sites it is intended to fill. Future work will investigate charge injection in a more highly radiation damaged CCD using an X-ray source to observe the effect of large numbers of radiation induced bright pixels on the ability of charge injection to reduce CTI. Further devices will also be studied to develop an understanding of the column to column non-uniformity in the size of the injected signal and to investigate the characteristics of different charge injection structures for potential application in CCDs for the ESA cornerstone mission, *GAIA*.

ACKNOWLEDGMENTS

The authors would like to thank E. Kendziorra and the staff at the Physikalisches Institut, Eberhard-Karls-Universität Tübingen, Germany for use of the Van de Graaff accelerator and proton damage beam line and e2v Technologies for supplying the CCD used for this work.

REFERENCES

1. A. D. Short, A. Keay, M. J. L. Turner, “Performance of the XMM EPIC MOS CCD detectors”, *Proc. SPIE*, vol. **3445**, (1998), pp. 13-27.
2. D. N. Burrows, J. E. Hill, J. A. Nousek, A. A. Wells, A. D. Short, R. Willingale, O. Citterio, G. Chincarini, G. Tagliaferri, S. Campana, “Swift X-ray telescope”, *Proc. SPIE*, vol. **4140**, (2000), pp. 64-75.
3. R. M. Ambrosi, A. D. T. Short, A. F. Abbey, A. A. Wells, D. R. Smith, “The effect of proton damage on the X-ray spectral response of MOS CCDs for the Swift X-ray Telescope”, *Nuc. Inst. Meth.*, vol. **A482**, (2002), pp. 644-52.
4. R. M. Ambrosi, D. R. Smith, A. F. Abbey, I. B. Hutchinson, E. Kendziorra, A. Short, A. Holland, M. J. L. Turner, A. Wells, “The impact of low energy proton damage on the operational characteristics of EPIC-MOS CCDs”, *Nuc. Inst. Meth.*, vol. **B207**, (2003), pp. 175-85.
5. S. Watts, A. Holmes-Siedle, A. Holland, “Further Radiation Evaluation of X-ray Sensitive Charge Coupled Devices (CCDs) for the XMM Telescope”, Brunel University Report, BRUCRD-ESACCD-95-1R, ISBN: 1872166148, (1995).
6. D. R. Smith, A. D. Holland, M. S. Robbins, R. M. Ambrosi, I. B. Hutchinson, “Proton induced leakage current in CCDs”, *Proc. SPIE*, vol. **4851**, (2003), pp. 842-48.
7. D. R. Smith, A. D. Holland, I. B. Hutchinson, “Random Telegraph Signals in Charge Coupled Devices”, in press, *Nuc. Inst. Meth.*, vol. **A**, (2004).